JACS
JOURNAL OF THE AMERICAN CHEMICAL SOCIETY

Communication

pubs.acs.org/JACS

Self-Assembly of Graphene Single Crystals with Uniform Size and Orientation: The First 2D Super-Ordered Structure

Mengqi Zeng,[†,§] Lingxiang Wang,[†,§] Jinxin Liu,[†] Tao Zhang,[†] Haifeng Xue,[†] Yao Xiao,[†] Zhihui Qin,[*,‡] and Lei Fu[*,†]

[†]College of Chemistry and Molecular Science, Wuhan University, Wuhan 430072, P. R. China

[‡]State Key Laboratory of Magnetic Resonance and Atomic and Molecular Physics, Wuhan Institute of Physics and Mathematics, Chinese Academy Sciences, Wuhan 430071, P. R. China

Supporting Information

ABSTRACT: The challenges facing the rapid developments of highly integrated electronics, photonics, and microelectromechanical systems suggest that effective fabrication technologies are urgently needed to produce ordered structures using components with high performance potential. Inspired by the spontaneous organization of molecular units into ordered structures by noncovalent interactions, we succeed for the first time in synthesizing a two-dimensional superordered structure (2DSOS). As demonstrated by graphene, the 2DSOS was prepared via self-assembly of high-quality graphene single crystals under mutual electrostatic force between the adjacent crystals assisted by airflow-induced hydrodynamic forces at the liquid metal surface. The as-obtained 2DSOS exhibits tunable periodicity in the crystal space and outstanding uniformity in size and orientation. Moreover, the intrinsic property of each building block is preserved. With simplicity, scalability, and continuously adjustable feature size, the presented approach may open new territory for the precise assembly of 2D atomic crystals and facilitate its application in structurally derived integrated systems.

As Arthur C. Clarke said, "Any smoothly functioning technology will have the appearance of magic". In the past few decades, materials with specific assembled structures have always caught our imagination for their derived wonderful properties.[1] Self-assembly allows for the integration of individual components and contributes to pattern formation, ordered objects, and functional systems with efficiency and simplicity. In recent years, the unique physicochemical properties of graphene triggered a great deal of attention toward two-dimensional (2D) materials.[2] The assembly of 2D single crystals into a superordered structure (SOS) in two dimension with tunable periodicity (including crystal size, spacing, orientation, etc.) is highly desirable. It will accelerate the integration of electrical and optical devices. With graphene as an example, a graphene SOS (GSOS) can serve as a conductive interconnection in integrated electronic circuits for barrier-free transparent contacts.[3] Graphene can also act as a component for hyperbolic metamaterials to achieve mild-infrared operation and thus can be assembled into optical elements.[4] What is more, when developing SOS composed by other 2D materials with a desired property or creating 2DSOS heterostructures,[5] the integration and combination of more interesting and exciting applications can be expected. However, the effective self-assembling of high-quality 2D crystals into superordered structures still remains unexplored.

For the chemical vapor deposition (CVD) of graphene single crystals on traditional solid substrates, such as commonly used Cu foil, their effective self-assembly seems impossible. Nucleation on solid metal catalysts is random, and subsequent growth tends to happen at fixed initial nucleation sites. However, the self-assembly growth of carbon nanotubes (CNTs) provides us inspiration. By using flow fluctuation in the CVD process, the self-assembling of CNTs into arrays can be easily achieved.[6] In this situation, it is the suspended state of the CNTs' mainbody in the airstream that ensures their self-assembly, whereas in the case for CVD grown graphene single crystals, they are closely attached to the solid substrate. Thus, changing the phase state of the growth substrate from a solid to a rheological liquid will be an artful choice to achieve their self-assembly. It has been reported that liquid fluidity of the catalyst could benefit the dispersion of graphene single crystals to some extent.[7] However, limited by uncontrollable kinetic factors, the produced graphene single crystals usually fail to exhibit uniform size and align in a predetermined manner. What is more, the ordered assembly behavior is easy to be terminated due to randomly generated new-born crystals resulted from the lack of preset nucleation sites.

Here, using graphene, the first identified 2D atomic crystal, we succeed for the first time in synthesizing 2DSOS. The graphene superordered structure (GSOS) was prepared via the self-assembly of high-quality graphene single crystals under a mutual electrostatic force between the adjacent crystals assisted by the airflow-induced hydrodynamic forces at the liquid metal surface. The synthesis strategy perfectly inherits the advantage of the traditional self-assembly method, which is both highly efficient and simple. The GSOS exhibits tunable periodicity in their spacing and outstanding uniformity in the size and orientation of the graphene crystals, which is, to the best of our knowledge, the first reported 2DSOS. We believe that the presented approach may open new territory for the precise assembly of 2D atomic crystals and facilitate their application in the structurally derived integrated systems.

Received: March 31, 2016
Published: June 17, 2016

DOI: 10.1021/jacs.6b03208
J. Am. Chem. Soc. 2016, 138, 7812−7815

The synthesis of GSOS, in brief, occurs as follows. PMMA is introduced as the solid carbon source serving as nucleation seeds, and it is spin-coated onto the Cu foil. As the temperature of the furnace is increased rapidly to the melting point of Cu in a H_2 atmosphere, the Cu foil melts, and the PMMA film decomposes and condenses; thus, nucleation seeds form. With an appropriate airflow with uniform speed and direction for disturbance, the original distribution of the seeds will be broken and the seeds tend to arrange in an energetically favorable way on the rheological surface, in which the spacing between the neighboring seeds will be nearly the same so as to balance evenly the whole energy on the liquid surface. Then CH_4 is introduced for the growth of the seeds. As the growth progresses, the mutual electrostatic force between the adjacent crystals continually increases, thus ultimately resulting in the formation of GSOS. Corresponding SEM images showing the self-assembly process of GSOS on liquid Cu are shown in Figure S1.

The distribution uniformity and quality of the as-prepared GSOS were evaluated, as shown in Figure 1. Figure 1a provides a

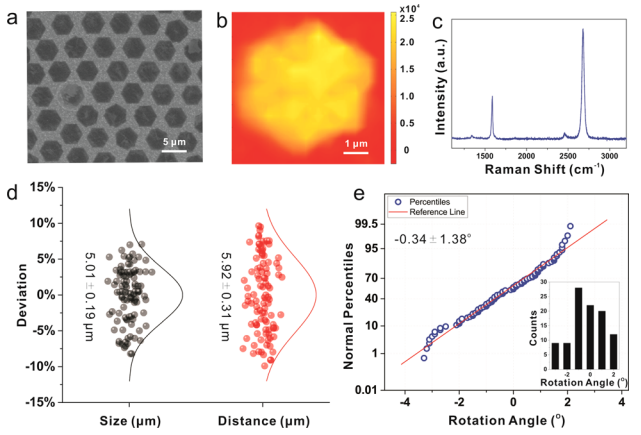

Figure 1. Characterizations of as-prepared GSOS. (a) SEM image of GSOS. (b) Raman mapping of the intensity of the 2D peak for an individual graphene single crystal. (c) Typical Raman spectrum of an individual graphene single crystal. (d) The statistical distribution about the deviation of size and distance of GSOS. (e) The percentile curve and (inset) histograms of the rotation angle of GSOS.

scanning electron microscopy (SEM) image of a typical GSOS. An array of graphene single crystals with uniform grain size was obtained, which may benefit from the uniform nucleation at the same time and the subsequent simultaneous growth of the seeds. Furthermore, the graphene single crystals exhibit a uniform distribution with a defined spacing over a large area. The edges of almost all the individual graphene single crystals are parallel in a line, which demonstrates the excellent orientation consistency of the GSOS. The entire array exhibits the characteristic features of a 2D superordered lattice structure. A typical Raman spectrum is also presented in Figure 1c. The typical intensity ratio (I_{2D}/I_G) within a grain is larger than 2, indicating that the samples are single-layer graphene. Moreover, the intensity of the D band (I_D) is negligible within the grain. A representative intensity mapping of 2D peak is plotted in Figure 1b for a hexagonal graphene grain. Grain boundaries do not appear to exist inside the grain, indicating the single crystal and high-quality aspects of the GSOS, which totally eliminates the nucleation marks reported in the traditional method using seeds to achieve the locating of graphene single crystals.[8] Our statistical study of over 100 sampling data collected from randomly selected graphene single crystals suggests that the GSOS has an extremely high uniformity and quality (see Figure S2). We consider these benefits arise from the "buffer effect" of the liquid metal catalyst for growing strictly monolayer graphene.[9] The statistical distribution of size and distance of graphene single crystals randomly selected over 1 cm^2 are shown in Figure 1d. The average value of the size and the distance of graphene grains are 5.01 and 5.92 μm, respectively. The corresponding standard deviations are 0.19 and 0.31 μm, respectively, which means that the deviation rates are 3.8% and 5.2%, respectively. The percentile function was employed to analyze the rotation angle distribution of GSOS, as shown in the histograms of Figure 1e. The normal percentile of the rotation angle was identified as conforming to a linear relationship. A preliminary view based on the above-mentioned statistical analysis suggests that the GSOS possess high consistency.

To further confirm the consistency of the GSOS at the microscale, scanning tunneling microscopy (STM) was employed. Two graphene single crystals (marked as c and e) were randomly selected from a 1 mm^2 GSOS region (Figure 2a).

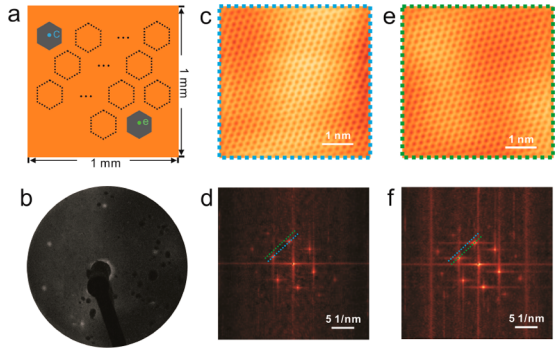

Figure 2. STM characterizations of as-prepared GSOS. (a) Two graphene single crystals (marked as c and e) were randomly selected from a 1 mm^2 GSOS region. (b) A typical LEED pattern of GSOS on Cu substrate. (c,e) STM images with atomic resolution of different graphene grains on Cu, revealing the clear honeycomb graphene structures. (d,f) The corresponding FFT results identified the consistent orientation of different graphene grains.

Two typical STM images were shown in Figure 2c,e, revealing the clear atomic resolution feature of honeycomb graphene structures. The corresponding 2D fast Fourier transformation (FFT) patterns (Figure 2d,f) identified the consistent orientation of GSOS.[10] More images with atomic resolution and the corresponding orientation exhibited by the FFT patterns at different regions are presented in Figure S3. They indicate that the orientations of the graphene single crystals in the GSOS are quite uniform. The STM images with atomic resolution over large collection areas are provided in Figure S4. They demonstrate the relatively good uniformity of the crystallographic orientation. Furthermore, low energy electron diffraction (LEED) was conducted at a sample with its size of ~1 × 1 cm^2, which is the maximum size for the sample holder in the STM, to confirm that graphene single crystals can really adjust their rotations on liquid Cu to achieve a high consistency in crystallographic orientation at the macroscale. A typical LEED pattern is shown in Figure 2b. The used electron energy was ~95 eV. The GSOS formed on the liquid substrate showed only one set of six bright diffraction spots, confirming the orientation consistency over a large area and thus proves the self-alignment of the graphene single crystals in GSOS.

DOI: 10.1021/jacs.6b03208
J. Am. Chem. Soc. 2016, 138, 7812−7815

It is worth noting that the size, spacing, and rotation angle of the graphene single crystals in GSOS can be precisely regulated by the gas flow rate, which can disturb the arrangement of the seeds. By varying the Ar flow rate in the annealing process we can obtain different GSOS on a melted Cu surface (Figure 3a–c), a

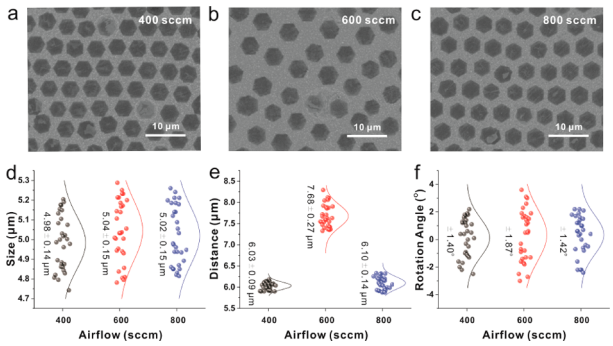

Figure 3. Controllable synthesis of GSOS via different flow rate. (a–c) SEM images of as-prepared GSOS. The Ar flow rate was 400, 600, and 800 sccm, respectively, in the annealing process. (d–f) Corresponding statistical distribution of the size, the distance, and the rotation angle of GSOS in a–c.

constant H_2 flow rate, and the same annealing time. The grain size, spacing, and rotation angle of the graphene single crystals in the GSOS for different air flows are statistically shown in Figure 3d–f. When the Ar flow rate is increased from 400 to 600 and 800 sccm, the sizes of the graphene grains are roughly maintained at 5 μm with tiny deviations since the subsequent growth conditions of the seeds are nearly the same. By adjusting the growth conditions, graphene single crystals with smaller or larger size can also be achieved. As for the spacing of graphene grains, it initially increases and then decreases with increasing the Ar flow rate. In addition, the standard deviation of rotation angles of graphene grains is less than 1.87° under these different Ar flow rates. An appropriate airflow favors the self-assembly of the graphene seeds. In our presented approach, by tuning the airflow, there is a precise regulation of the characteristic parameter of highly consistent GSOS, which is crucial for various applications in the structurally derived integrated systems. More GSOS with different distances and sizes are presented in Figures S5–S7 and the influence of each parameter is also systematically demonstrated.

The most fascinating feature of the presented approach is its precise control of the crystallographic orientation. The root cause lies in the electrostatic interaction of the as-grown graphene single crystals on the liquid metal catalyst. Static electricity is generated in the process of the growth of the graphene single crystals. The Window version of the Gaussian 09 (G09W) suite of programs was employed in this study. Molecular structures as well as the electrostatic potential (ESP) maps are determined. The results show that the edge of this structure has an anisotropic electrostatic potential distribution. The calculated ESP $Vs(r)$ on the molecular surface of these molecules is presented in Figure 4a. The larger the number of rings in an individual graphene single crystal unit, the more anisotropic the electrostatic potential distribution is, as shown in Figure S8. In each instance, $Vs(r)$ is negative over the whole graphene single crystal, while its values are different toward each side. Thus, owning to the directivity of the static electric field, each individual graphene single crystal tends to adjust its own orientation to match that with the neighboring

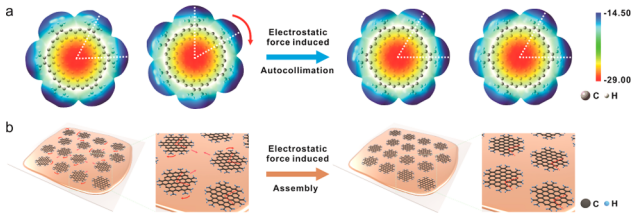

Figure 4. Schematic of the self-assembly mechanism of the graphene single crystals in order to form GSOS. (a) Electrostatic force induced autocollimation of the graphene single crystals. Structures and electrostatic potential distribution was clearly exhibited. (b) Schematic of the electrostatic interaction induced assembly of the graphene grains over a large area.

one. When it comes to a group of seed-prelocated graphene single crystals, each graphene single crystal in the array will try to rotate to match itself due to the anisotropic static electric field, as exhibited in Figure 4b. The rheological property of the underlying amorphous liquid substrate makes a self-adjusting rotation possible. In addition, what is worth noting is that the uniformity of the grain size in GSOS is important to the self-assembly induced by the static electric field. Since graphene single crystals obtained on the liquid surface have the same grain size, the value of the ESP $Vs(r)$ of each single crystal will be quite uniform. For an individual graphene single crystal, it will be exposed to a uniform electric field since the electrostatic repulsion at each direction will be the same. Therefore, via the precise control of the static electricity, the units of graphene single crystals tend to assemble into a superordered lattice structure with the same crystallization orientation, as shown in Figure 1a.

In addition, we also employed carbamide to act as the solid carbon source for the formation of the seeds in order to achieve the doping of the GSOS, as shown in Figure S9, which also possesses uniform size, spacing, and rotation angle. Thus, it is promising to achieve GSOS with adjustable properties to extend its future applications. The electrical performance of the GSOS was examined by constructing back-gated field-effect transistor (FET) array. The derived mobility is 3882 ± 896 cm^2 V^{-1} s^{-1}, which reflects the high quality of the GSOS (Figure S10b) and is comparable with that of the unassembled graphene single crystals (Figure S11). In addition, we employed GSOS as electrode pairs for connecting MoS_2 flakes, thus demonstrating its potential for building nanoscale device arrays (Figure S10d).

In brief, we have demonstrated an experimental pathway to obtain the GSOS with uniform size and orientation, that is the first 2D superordered structure via self-assembling process. The electrostatic interactions of the graphene single crystal facilitate the ultimate precise orientation with each other. The as-obtained 2DSOS exhibits tunable periodicity in space and outstanding uniformity in the size and orientation. Moreover, the intrinsic property of each building block can be preserved. The presented approach is scalable and cost-effective for the production of superordered structures. We believe it may open new territory of integrate units based on 2D nanomaterials with atomic thickness and extensively adjustable property, such as the optical and electrical elements in the future applications.

■ ASSOCIATED CONTENT

Supporting Information

The Supporting Information is available free of charge on the ACS Publications website at DOI: 10.1021/jacs.6b03208.

DOI: 10.1021/jacs.6b03208
J. Am. Chem. Soc. 2016, 138, 7812–7815

Experimental details and supplementary figures (PDF)

AUTHOR INFORMATION

Corresponding Authors

*leifu@whu.edu.cn

*zhqin@wipm.ac.cn

Author Contributions

§These authors contributed equally to this work.

Notes

The authors declare no competing financial interest.

ACKNOWLEDGMENTS

The research was supported by the Natural Science Foundation of China (Grants 51322209, 21473124) and the Sino-German Center for Research Promotion (Grant GZ 871).

REFERENCES

(1) (a) Altug, H.; Vuckovic, J. *Opt. Express* **2005**, *13*, 8819. (b) Kim, S.; Jeong, H. Y.; Kim, S. K.; Choi, S.-Y.; Lee, K. J. *Nano Lett.* **2011**, *11*, 5438. (c) Park, W. I.; You, B. K.; Mun, B. H.; Seo, H. K.; Lee, J. Y.; Hosaka, S.; Yin, Y.; Ross, C. A.; Lee, K. J.; Jung, Y. S. *ACS Nano* **2013**, *7*, 2651.

(2) (a) Kravets, V. G.; Grigorenko, A. N.; Nair, R. R.; Blake, P.; Anissimova, S.; Novoselov, K. S.; Geim, A. K. *Phys. Rev. B: Condens. Matter Mater. Phys.* **2010**, *81*, 155413. (b) Song, Y.; Fang, W.; Brenes, R.; Kong, J. *Nano Today* **2015**, *10*, 681. (c) Bhimanapati, G. R.; Lin, Z.; Meunier, V.; Jung, Y.; Cha, J.; Das, S.; Xiao, D.; Son, Y.; Strano, M. S.; Cooper, V. R.; Liang, L.; Louie, S. G.; Ringe, E.; Zhou, W.; Kim, S. S.; Naik, R. R.; Sumpter, B. G.; Terrones, H.; Xia, F.; Wang, Y.; Zhu, J.; Akinwande, D.; Alem, N.; Schuller, J. A.; Schaak, R. E.; Terrones, M.; Robinson, J. A. *ACS Nano* **2015**, *9*, 11509.

(3) Liu, Y.; Wu, H.; Cheng, H. C.; Yang, S.; Zhu, E.; He, Q.; Ding, M.; Li, D.; Guo, J.; Weiss, N. O.; Huang, Y.; Duan, X. *Nano Lett.* **2015**, *15*, 3030.

(4) Chang, Y. C.; Liu, C. H.; Liu, C. H.; Zhang, S.; Marder, S. R.; Narimanov, E. E.; Zhong, Z.; Norris, T. B. *Nat. Commun.* **2016**, *7*, 10568.

(5) (a) Xie, L. M. *Nanoscale* **2015**, *7*, 18392. (b) Balendhran, S.; Walia, S.; Nili, H.; Sriram, S.; Bhaskaran, M. *Small* **2015**, *11*, 640.

(6) Wei, D. C.; Liu, Y. Q.; Cao, L. C.; Fu, L.; Li, X. L.; Wang, Y.; Yu, G.; Zhu, D. B. *Nano Lett.* **2006**, *6*, 186.

(7) (a) Geng, D.; Wu, B.; Guo, Y.; Huang, L.; Xue, Y.; Chen, J.; Yu, G.; Jiang, L.; Hu, W.; Liu, Y. *Proc. Natl. Acad. Sci. U. S. A.* **2012**, *109*, 7992. (b) Geng, D.; Luo, B.; Xu, J.; Guo, Y.; Wu, B.; Hu, W.; Liu, Y.; Yu, G. *Adv. Funct. Mater.* **2014**, *24*, 1664.

(8) Wu, W.; Jauregui, L. A.; Su, Z.; Liu, Z.; Bao, J.; Chen, Y. P.; Yu, Q. *Adv. Mater.* **2011**, *23*, 4898.

(9) (a) Wang, J.; Zeng, M.; Tan, L.; Dai, B.; Deng, Y.; Rummeli, M.; Xu, H.; Li, Z.; Wang, S.; Peng, L.; Eckert, J.; Fu, L. *Sci. Rep.* **2013**, *3*, 2670. (b) Zeng, M.; Tan, L.; Wang, J.; Chen, L.; Rümmeli, M. H.; Fu, L. *Chem. Mater.* **2014**, *26*, 3637. (c) Tan, L.; Zeng, M.; Zhang, T.; Fu, L. *Nanoscale* **2015**, *7*, 9105.

(10) Horcas, I.; Fernandez, R.; Gomez-Rodriguez, J. M.; Colchero, J.; Gomez-Herrero, J.; Baro, A. M. *Rev. Sci. Instrum.* **2007**, *78*, 013705.

DOI: 10.1021/jacs.6b03208
J. Am. Chem. Soc. 2016, 138, 7812−7815